HHS Public Access

Author manuscript

Oncogene. Author manuscript; available in PMC 2016 August 15.

Published in final edited form as:

Oncogene. 2016 August 11; 35(32): 4256–4268. doi:10.1038/onc.2015.491.

YB-1 is elevated in medulloblastoma and drives proliferation in Sonic hedgehog - dependent cerebellar granule neuron progenitor cells and medulloblastoma cells

Abhinav Dey[1], **Mélanie Robitaille**[2,Ψ], **Marc Remke**[3,Ψ], **Caroline Maier**[1], **Anshu Malhotra**[1], **Alex Gregorieff**[4], **Jeffrey L Wrana**[4], **Michael D Taylor**[3], **Stéphane Angers**[2], and **Anna Marie Kenney**[1,*]

[1]Department of Pediatric Oncology, Emory University, Atlanta, GA 30322, USA

[2]Department of Pharmaceutical Sciences, Leslie Dan Faculty of Pharmacy, University of Toronto, Toronto, Ontario M5S 3M2, Canada. Department of Biochemistry, Faculty of Medicine, University of Toronto, Toronto, Ontario M5S 1A8, Canada

[3]The Arthur & Sonia Labatt Brain Tumour Research Center, Hospital for Sick Children, Toronto, ON M5G-1X8 Canada

[4]Center for Systems Biology, Samuel Lunenfeld Research Institute, Mount Sinai Hospital, Toronto, Ontario M5G 1X5, Canada

Abstract

Post-natal proliferation of cerebellar granule neuron precursors (CGNPs), proposed cells-of-origin for the SHH-associated subgroup of medulloblastoma (MB), is driven by Sonic Hedgehog (Shh) and Insulin-like Growth Factor (IGF) in the developing cerebellum. Shh induces the oncogene Yes-associated protein (YAP), which drives IGF2 expression in CGNPs and mouse Shh-associated medulloblastomas. To determine how IGF2 expression is regulated downstream of YAP, we carried out an unbiased screen for transcriptional regulators bound to IGF2 promoters. We report that Y-box binding protein-1 (YB-1), an onco-protein regulating transcription and translation, binds to IGF2 promoter P3. We observed that YB-1 is up-regulated across human medulloblastoma subclasses as well as in other varieties of pediatric brain tumors. Utilizing the cerebellar progenitor model for the Shh-subgroup of MB in mice, we show for the first time that YB-1 is induced by Shh in CGNPs. Its expression is YAP-dependent and it is required for IGF2 expression in CGNPs. Finally, both gain-of function and loss-of-function experiments reveal that

*Author for correspondence (anna.kenney@emory.edu).
Ψthese authors equally contributed to this work

Competing interests
The authors declare no competing financial interests.

Author Contributions
A.D. and A.M.K. designed the research. A.D., M.R.[2], M.R.[3], C.M. and A.M. performed the experiments and analyzed the data. A.G. and J.L.W. provided YAP(LoxP) mice and assisted with their husbandry. M.R[2], M.R.[3], J.L.W., M.D.T., S.A. edited the manuscript prior to submission. A.D. and A.M.K. wrote the paper. All authors read and commented on the manuscript and approved the final version.

Supplemental Information accompanies the paper on the *Oncogene* website (http://www.nature.com/onc)

YB-1 activity is required for sustaining CGNP and medulloblastoma cell (MBC) proliferation. Collectively, our findings describe a novel role for YB-1 in driving proliferation in the developing cerebellum and medulloblastoma cells and they identify the SHH:YAP:YB1:IGF2 axis as a powerful target for therapeutic intervention in medulloblastomas.

Keywords

Medulloblastoma; Sonic hedgehog; Hippo; YB1; YAP; IGF2; cerebellum; cell cycle

Introduction

Medulloblastoma (MB) accounts for 25% of primary central nervous system (CNS) neoplasms in the pediatric age range (1). Medulloblastomas can be divided into 4 genetically and histologically defined subgroups (2–4). Certain subgroups are marked by up-regulation of expression of Sonic hedgehog (Shh) or Wnt pathway targets, and others are marked by amplification or up-regulation of *MYC* ("Group C") and the presence of isochromosome 17q ("Group D").

Shh-associated MB is proposed to arise from neural precursors in the rhombic lip (5). These cells, cerebellar granule neuron precursors (CGNPs), are destined to form the external granular layer (EGL) of the cerebellar cortex, where they will undergo a period of rapid, Shh-induced proliferation. The Shh ligand, secreted by Purkinje neurons, interacts with the 12-transmembrane domain receptor Patched (Ptc), which inhibits Smoothened (Smo), a 7-pass transmembrane protein. Shh interaction with Ptc relieves the inhibition of Smo, resulting in pathway activation and nuclear translocation of Gli family transcription factors, which activate target genes driving CGNP proliferation and inhibiting differentiation (6–8).

Importantly, primary cultures of CGNPs can be derived from post-natal (PN) 4/5 mice and maintained in a proliferative state for ~72 hours by the addition of exogenous Shh protein. Thus, primary CGNP cultures are an excellent system for isolating and studying Shh mitogenic signaling and interactions with other pathways, including the insulin-like growth factor (IGF) pathway, which cooperates with Shh at multiple levels during normal cerebellar development and in medulloblastoma (9–14). Unlike other tumor subgroups, SHH MBs have been straightforward to model in mice by deletion of Ptc, or by activation of Smo. We utilize a mouse model developed by Jim Olson (Fred Hutchinson Cancer Research Center). These mice express an activated mutant allele Smoothened (SmoA1) (a G-protein coupled receptor that is critical for Shh pathway activation) under the control of NeuroD2 promoter (15).

Previously, we investigated interactions between Shh signaling and the tumor-suppressive Hippo pathway in the developing cerebellum and Shh-associated medulloblastomas. We showed that Shh induces Yes-Associated protein-1 (YAP) expression in CGNPs, and YAP can drive CGNP proliferation, even in the absence of Shh. In humans, YAP and TEAD1 are most highly expressed in the Shh and Wnt subclasses (10). Additionally we showed (12), that mice implanted with YAP-expressing tumor cells succumbed more rapidly than control mice who received GFP-transduced medulloblastoma cells. After whole body irradiation,

YAP-transduced tumors featured proliferating cells, suggesting that the tumor cells had not undergone radiation-induced growth arrest. When YAP-infected CGNPs were irradiated, they resolved DNA damage-induced foci more rapidly, but this was not due to more efficient DNA repair. Rather, YAP-expressing CGNPs inactivated the Chk2/ATM DNA damage response pathway, resulting in abrogation of the G2M-phase cell cycle checkpoint. We showed that this effect of YAP was a result of YAP-mediated induction of *IGF2*. Importantly, in human medulloblastoma patient samples, IGF2 was most highly expressed in the SHH subtype, and knocking down IGF2 in YAP-transduced cells rescued the appropriate response to irradiation (12).

To further understand how IGF2 expression is regulated in medulloblastoma cells and Shh-responsive CGNPs, we carried out an unbiased screen for transcriptional regulators bound to the IGF2 promoter 3 (P3), which drives IGF2 expression in the developing brain and in medulloblastomas (16). Using mass spectrometry, we identified several potential regulators of IGF2 expression that could be functioning along with, or downstream of YAP. One of these factors is Y-box protein-1 (YB-1), which due to its implication in many cancer-associated cellular programs, such as cell proliferation, genomic instability, angiogenesis, invasion, metastasis, and inflammation (17), attracted our interest. YB-1 is overexpressed in many malignancies, including colorectal carcinomas (18), prostate cancer (19), osteosarcoma (20), ovarian serous adenocarcinoma (21, 22), lung cancer (23, 24), synovial sarcoma (25) and breast cancer (26–30). However, much less is known about the role of YB-1 in childhood cancers. The first report showing that YB-1 is a feature of pediatric glioblastoma multiforme (GBM) was published in 2007 (31). Here, we report for the first time that YB-1 is up-regulated in all subclasses of medulloblastomas. We observed that YB-1 is required for proliferation in CGNPs and medulloblastoma cell (MBC) cultures, and also in a 3-dimensional context of cerebellum and tumors using an organotypic slice culture-based approach. We also demonstrate that YB-1 is required for IGF2 expression in CGNPs, and it is a YAP-dependent target of Shh signaling in cerebellar granule neural precursors (CGNPs). Taken together, these findings point to YB-1 as an essential regulator of CGNP and medulloblastoma cell proliferation, suggesting the YAP: YB-1:IGF2 axis as a novel target that may block tumor growth in SHH-associated medulloblastoma.

Results

YB-1 is highly expressed in all subclasses of human medulloblastomas

We have previously observed IGF2 expression driven by YAP (12), a target of Shh in primary CGNP cultures (10), but the mechanism through which this occurs remained unclear. Regulation of IGF2 expression is extremely complex. In most tissues, the maternal copy of the *IGF2* gene is imprinted, and transcription takes place from the paternal copy. Moreover, there are 4 *IGF2* promoters, from which tissue-specific transcription takes place. In the human fetal brain, there is loss of *IGF2* imprinting, and in regions such as the choroid plexus, transcription takes place from both alleles, using promoter P3 (32). In human medulloblastomas of all classes, promoter P3 most strongly drives *IGF2* expression (33). We wanted to determine whether YAP directly regulates IGF2 expression, or whether another protein intermediate is required. To this end, we employed biotinylated-DNA ‘fishing’

combined with mass spectrometry (34) (35) to delineate the transcriptosomes (36) at the IGF2 promoters. The IGF2 promoters have already been mapped in mouse (37) and analysis of the promoter usage in the developing mouse cerebellum showed promoter P3 being predominant over promoter P1 (16). We designed primers specific for promoters P3 and P1 with a biotin-tag at the 5′ end of the forward primer (Supplementary Table S1). The respective promoter regions were PCR amplified from mouse genomic DNA and gel purified. The amplicons were incubated with streptavidin coated magnetic beads and subsequently mixed with lysates enriched in nuclear proteins from PZp53Med cells- a line derived from a medulloblastoma arising in a $Ptc^{+/-}/p53^{-/-}$ mouse (38)- and SmoA1 tumor tissue. The eluates were subjected to mass spectrometry analysis to identify proteins bound to the respective promoters. The mass spectrometry results showed YB-1 protein associated with IGF2 promoter P3 in nuclear-fraction enriched lysates from both SmoA1 tumor and PZp53Med cell line (Supplementary Table S2; Supplementary Figure S1a and b). The mass spectrometry data for YB-1 was reconfirmed by western blot for YB-1 in the eluates from the same experiment (Supplementary Figure S1c and d). However, these results for YB-1 were obtained in a mouse model and in a cell line derived from a mouse medulloblastoma. It was therefore imperative to search for the association of YB-1 with medulloblastoma in human samples.

A role of YB-1 in medulloblastoma has not been elucidated, thus we determined the gene expression pattern of YB-1 in a human medulloblastoma cohort comprising of >200 samples (39). We observed YB-1 up-regulation in all four subclasses of medulloblastoma (Figure 1a) as compared to normal cerebellar controls. A similar trend in gene expression was observed for a smaller cohort of 64 samples of medulloblastomas (Supplementary Figure S2a) (3). The difference in gene expression was analyzed using one way ANOVA and was found to be significant ($p<0.001$) (Figure 1a). Focal amplification and copy number gains harbouring *YBX1* were observed in 4 out of 1088 medulloblastomas, all of which belonged to the SHH subgroup (Figure 1b). The list of genes found in the amplified locus of Chr1 (Figure 1b) and sharing the locus with *YBX1* includes transcription factors such as FoxJ3 and translation-associated genes like RIMKLA, which co-relate with the role of YB-1 as a transcription-translation factor.

The role of aberrant activation of extra-cellular signaling pathways as a mechanism of YB-1 upregulation in medulloblastomas remains unexplored. As mentioned previously, the Shh subgroup of MB has already been modeled in mice by deletion of Ptc, or by activation of Smo. Additionally, we detected YB-1 associated with IGF2 promoter P3 in a cell line and primary tumor tissue derived from these mouse models. Our previous studies have shown YAP-mediated activation of IGF2 as radiation resistance mechanism specific to the Shh-subgroup of MB due to uniquely high mRNA levels of YAP and IGF2 in these samples (10, 12). Taken together, these observations are suggestive of a distinct role of YB-1 in Shh subgroup of MB. We carried out immunostaining for YB-1 on a tumor section derived from Shh-subgroup human MB and found it to be positively stained for YB-1 (Supplementary Figure S2b). We confirmed specificity of the YB-1 antibody using peptide competition (Supplementary figure S2c). After confirming the presence of YB-1 protein in Shh-subgroup human MB, we next wanted to determine the role played by YB-1 in Shh-driven proliferation.

YB-1 is a target of Shh-signaling and controls proliferation in CGNPs

CGNPs in the developing cerebellum depend upon Shh signaling for proliferation and are believed to be the cell-of-origin for SHH-associated medulloblastomas. These cells require IGF2 signaling for their survival through the PI3K-Akt signaling pathway (12, 40), and we have previously shown that mitogenic Shh signaling cooperates with the IGF2 pathway at a number of levels (9, 11, 13). Having observed that YB-1 binds the IGF2 promoter in SmoA1 and Pzp53med cells, we next asked whether YB-1 is itself a target of mitogenic Shh signaling. We prepared whole cell extracts from primary CGNP cultures grown in absence of serum and treated with purified Shh protein, versus Shh-vehicle. Upon analyzing CGNP protein lysates by western blotting after 48 h of Shh treatment, we observed high levels of YB-1 protein (Figure 2a). In order to gain additional insight into the mechanism through which Shh regulates YB-1, we treated CGNPs with the Smoothened inhibitor cyclopamine (38) for 12h. This attenuated the Shh-induced increase in YB-1 protein (Figure 2a). Immunofluorescence analysis indicates that YB-1 is present in CGNPs undergoing proliferation, as determined by colocalization with the proliferation marker Ki67 (Figure 2b, c). However, we did not observe any significant change in mRNA levels (Figure 2d), which is indicative of a post-transcriptional mechanism for up-regulation of YB-1 downstream of Shh in CGNPs.

Mitogenic Shh signaling directs CGNPs to stay in the cell cycle and when Shh is withdrawn, these cells terminally exit the cell cycle within six hours (41). The downstream targets of Shh mitogenic signaling include *Gli1, Gli2, N-myc, YAP, and IRS*-1 (10, 11, 42–44). YB-1 has been shown to be an activator of several genes involved in proliferation including DNA polymerase α (45) and PCNA (23). Since YB-1 is induced by Shh in CGNPs, we wished to determine whether manipulation of YB-1 levels affected proliferation in presence of Shh. We overexpressed YB-1 in CGNPs and observed the levels of Cyclin D2 and Ki67-positive CGNPs increased as a result (Figure 3a, b and b′). The efficiency of adenoviral infection was verified using quantification of GFP positive CGNPs post-infection as the adenoviral construct for YB-1 had GFP cloned with an independent promoter (Supplementary Figure S3a). We subsequently carried out loss-of-function analysis using lentiviruses carrying short hairpin RNA (shRNA) sequences targeting YB-1. YB-1 was targeted by five shRNA clones and we found that three out of five shRNA lentiviruses tested in on CGNPs were effective in knocking down YB-1 (Supplementary Figure S4a; Supplementary Table S3). For a control an shRNA that had a scrambled RNA targeting sequence was used. We observed decreased levels of Cyclin D2 in YB-1-knocked down CGNPs (Figure 3c), without any decrease in survival (as indicated by cleaved-caspase3 levels). To rule out off-target effects, we used another verified shRNA construct (Lenti 1; Supplementary Table S3) against YB-1 and compared it with the construct used in this study to knockdown YB-1. This construct (Lenti1) did not target YB-1 and CycD2 in CGNPs, but the construct used in our study did knock down YB-1 and reduce CycD2 levels in CGNPs (Supplementary Figure S4b). Quantitative determination of the effect of YB-1 loss on proliferation was determined by measurement of PCNA positive cells in control versus YB-1 shRNA-infected cells following 72hr incubation in the presence of Shh (Figure 3d). The number of PCNA positive cells was reduced by 70% in YB-1 targeted CGNPs as compared to Shh-treated control shRNA-

infected CGNPs, as determined by quantification of immunofluorescent staining ($p<0.001$) (Figure 3e).

It is important to study the role of genes regulating CGNP proliferation in context of other cell types present in the developing cerebellum, as cell-cell signaling and maintenance of tissue architecture are essential for correct development, and these nuances are lost in dissociated monolayer cultures. Unfortunately, YB-1-null mice do not survive post-natally (46) and to date no YB-1 conditional alleles have been reported. Since the CGNPs proliferate *in vivo* in the external granular layer of the developing postnatal cerebellum, we performed immunofluorescent staining of mouse cerebellar sections at three developmental stages: postnatal day7 (PN7), at the peak of CGNP proliferation; PN15, when proliferation is diminishing; and adulthood, when cerebellar development reaches completion. YB-1 expression was evident in the EGL during the peak of CGNP proliferation (Figure 4a and b) at PN7. However, at P15 YB-1 was present in granule cells in the IGL, as well as their processes in the molecular layer. The expression of YB-1 was negligible in the adult cerebellum. Similar observations have been previously made regarding the age dependent expression of YB-1 in mice (47). Our results indicate that YB-1 protein is associated with CGNPs undergoing proliferation induced by Shh *in vitro* and *in vivo*, and that YB-1 could be playing other roles in subsequent stages of cerebellar development.

YB-1 co-expressed with PCNA positive cells in the EGL of P7 mouse cerebella (Figure 4b). Therefore, to evaluate the requirement for YB-1 in CGNPs proliferating in context of their microenvironment, we used cerebellar organotypic cultures. Cerebellar slices from P5 SW129 wild type mice were electroporated with plasmids for non-targeting ScrShRNA or with YB-1-targeting ShRNA constructs. After 4 days in culture, the cerebellar slices were fixed and stained for Ki67. Upon confocal imaging, we observed that the EGL stained strongly for Ki67 in cerebellar slices treated with ScrShRNA in comparison to the slices treated with YB-1-shRNA or cerebellar slices grown in the absence of Shh (Figure 4 c,d). The electroporation of GFP expressing lentiviral plasmid was used as a control to verify the efficiency of electroporation (Supplementary Figure S5). These results demonstrate a requirement for YB-1 in CGNP proliferation in vitro and in context of an intact cerebellar environment *ex vivo*.

YB-1 regulates Igf2 expression and it is a target of YAP in CGNPs

YB-1, bound to promoters of various genes, has been known to be a transcriptional activator or repressor in a context dependent manner (17, 48). It has been shown previously that YB-1 binds to the IGF2 promoter by ChIP-on-chip analysis in breast cancer cells (49). We further validated the promoter-binding data using chromatin immunoprecipitation (ChIP) experiments to scan for YB-1 binding sites on *Igf2* promoter. An electronic search on the eukaryotic promoter database (http://epd.vital-it.ch/) revealed three YB1-binding sites in the 5000 bp region upstream of transcription start site of the Shh effector Igf2 (Supplementary Figure S6). As shown in Figure 5a and 5b, we found statistically significant evidence that YB-1 binds to two out of the three YB-1-binding sites that we analyzed on the *Igf2* promoter. Thus, we wished to determine whether YB-1 binds to IGF2 promoter P3 in Shh-induced CGNPs. We carried out the same biotinylated DNA binding analysis of IGF2

promoters we earlier showed in figure S1, this time using lysates from Shh-induced CGNPs and found that YB-1 was bound to IGF2 promoter P3 (Figure 5c).

It is not known whether YB1 acts as an activator or repressor of IGF2 expression. To determine the role of YB-1 in regulating IGF2 expression we knocked down YB-1 using shRNA-carrying lentiviruses as described above in Shh-treated CGNPs and measured the mRNA from IGF2 promoter P3 by quantitative reverse transcription-polymerase chain reaction (RT-PCR). We found that IGF2 mRNA expression decreased significantly in the CGNPs with YB-1 knocked down (Figure 5d). Taken together, these observations suggest that YB-1 is essential for IGF2 expression in CGNPs. Arguably, however, the effect of YB1 knockdown in IGF2 expression could merely be the result of affecting activity of a major transcriptional regulator. To determine whether manipulation of YB1 broadly affects other genes downstream of Shh signaling, we searched for other genes that are associated with Shh signaling and have been reported to be transcriptionally associated with YB-1 based on a recent ChIP-on-Chip analysis (49). We that found NMyc (44), Bcl6 (50), Mtss1 (51) and Gli1 (52) met these criteria. We next over-expressed YB-1 and GFP in CGNPs initially primed with Shh and then grown in absence of Shh post-transduction, to identify the role YB-1 plays in driving the expression of these genes. We found that neither Gli1 mRNA nor did NMyc mRNA levels showed any significant change, (Supplementary figure S7), suggesting they are regulated independently of YB1 activity. On the other hand the levels of tumor suppressor Bcl6 and Mtss1 mRNA were significantly lowered. Therefore, two of the known Shh targets (NMyc and Gli1) were not affected by overexpression of YB-1 while the other two Bcl6 and Mtss1 were down-regulated. These results indicate that manipulation of YB1 activity has effects on specific targets, such as IGF2, and does not cause general alterations of gene expression.

We have previously established YAP as a downstream target of Shh and an upstream regulator of IGF2 (10, 53). The findings described above show that IGF2 expression also lies downstream of YB1. We thus wished to determine whether YAP is an upstream regulator of YB1 levels. To this end, we isolated CGNPs from P5 cerebella of YAP-*loxP* mice (gift of Jeff Wrana, The Lununfeld-Tanenbaum Research Institute, Canada) (54) and infected them with adenoviruses expressing Cre-recombinase (Vector Biolabs), or control GFP adenoviruses (Supplementary Figure S4b). After 48 hours (post-infection), the cells were lysed and the lysates were probed by western blotting. Figure 5e shows that Cre-mediated ablation of YAP from CGNPs down-regulates cyclin D2 consistent with our previous report that YAP is required for Shh-driven CGNP proliferation. Moreover, Cre-mediated YAP ablation also blocked YB-1 induction. These results show that YAP is an upstream regulator of YB-1 expression in CGNPs.

YB-1 controls proliferation of SmoA1 medulloblastoma cells and tissues

To determine whether the up-regulated levels of YB-1 in Shh-stimulated CGNPs are conserved in Shh-mediated tumorigenesis, we analyzed its levels in medulloblastomas harvested from SmoA1 mice in comparison with adjacent, non-tumor cerebellar tissue. As shown in Figure 6a and b, the tumor tissue exhibited higher levels of YB-1 protein as compared to adjacent cerebellar tissue. Next, we wanted to determine if YB-1 plays a role in

regulating proliferation of MB cells (MBCs) with constitutively active Shh pathway. Thus, we cultured MBCs derived from SmoA1 medulloblastomas and infected them with adenoviruses expressing GFP versus YB-1/GFP (at similar levels of infectivity; see Supplementary Figure S8) as well as lentiviruses expressing YB-1 targeting shRNA versus Scr-shRNA. The results in MBCs were consistent with the effect of YB-1 knockdown and overexpression in Shh-induced CGNPs. The MBCs overexpressing YB-1 showed increased levels of CycD2 (Figure 6c) and while shRNA-mediated knock down of YB-1 reduced CycD2 levels, without any change in cell-survival (based on cleaved caspase-3 levels) (Figure 6d). We observed that SmoA1 tumor tissue features cells with higher levels of YB-1 co-expressing with PCNA (Figure 6b) when compared with adjacent non-tumor tissue. To ascertain the requirement for YB-1 in cell proliferation in the tumor microenvironment, we electroporated the SmoA1 tumor slice cultures with lentiviral plasmids encoding non-targeting ScrShRNA or YB-1-targeting ShRNA. The efficiency of electroporation was judged by electroporating an GFP expressing lentiviral plasmid (pLKO-GFP) (Supplementary Figure S9). The slice cultures were then immunostained for cell proliferation marker Ki67 to determine the effect of YB-1 knockdown on proliferation. The results of confocal imaging for the tumor regions showed that there was a substantial decrease of PCNA staining in slice cultures with YB-1 knocked-down (Figure 6e, f). These results indicate that down-regulation of YB-1 levels in the cells and tissues derived from SmoA1-medulloblastoma can reduce proliferation. Additionally, we determined the IGF2 mRNA levels from MBC cultures expressing shRNA targeting YB-1 (Supplementary Figure S10) and found them to be significantly reduced when compared to control.

Discussion

YB-1 is an oncogenic transcription/translation factor and its activity leads to the development of cancer (55). The first report associated with YB-1 in pediatric brain tumors showed that it is overexpressed in pediatric glioblastomas (31). During embryonic development, the role of YB-1 has been proven to be essential (46) as it contributes to neural tube closure and cell proliferation. The expression of YB-1 closely correlates with cell proliferation state during mammalian development (47, 56) and decreases steadily during development. In spite of such knowledge, there is a lack of understanding how or which extra-cellular signals induce YB-1 expression in proliferating undifferentiated cells during development. The known extracellular signals controlling YB-1 expression in differentiated cells include interleukin-2 in T-helper lymphocytes (57), serum-activated fibroblasts (58) and thrombin in endothelial cells (59).

Our observation of induction of YB-1 by Shh and its inhibition by Cyclopamine (SmoA1-antagonist) in CGNPs, putative cells of origin for the SHH-associated subgroup of medulloblastomas, confirmed that YB-1 is a target of canonical Shh mitogenic signaling in the developing cerebellum. The Shh-induced CGNPs that were positive for YB-1 were also positive for PCNA, indicating the correlation between YB-1 overexpression and cell proliferation in progenitor cells. The co-expression of YB-1 with PCNA in the EGL is indicative of the active role played by YB-1 in proliferative regions of the cerebellum controlled by Shh *in vivo*. The knockdown of YB-1 dramatically reduced the CGNP proliferation and its over expression led to increased proliferation. Moreover, our results

show that knockdown of YB-1 in organotypic cerebellar slices reduced the thickness of EGL as well as the number of proliferative cells, emphasizing that the proliferative effect of YB-1 is maintained in a cerebellar macroenvironment, which preserves several important architectural features of the host tissue, such as neuronal connectivity, cellular stoichiometry and glial–neuronal interactions (60). Taken together, our results indicate that YB-1 protein is associated with CGNPs undergoing proliferation induced by Shh *in vitro,* and *ex vivo*, and that YB-1 could be playing other roles in subsequent stages of cerebellar development, a matter for future investigation.

We identified YB-1 interacting with IGF2 promoter P3 in the lysates from Shh-induced CGNPs. Although YB-1 has been reported to interact with the IGF2 promoter in breast cancer cells (49), there have been no further reports that analyze the functional aspect of this association in developmental and oncogenic pathways in the cerebellum. Although IGF2 expression is detectable at the two-cell stage and is strong in extra-embryonic tissues as early as embryonic day 4.5 (E4.5), expression in the embryo is not evident until E7.5, increasing rapidly thereafter (61). IGF2 is expressed in the developing and mature cerebellum. Thus, YB-1 can be a positive or a negative regulator of transcription for *IGF2,* as has been the case for multiple gene promoters that house Y-box sequences (TAACC) (62–67). We knocked-down YB-1 in CGNPs and observed a corresponding decrease in IGF2 mRNA levels indicative of the activational role played by YB-1 in regulating IGF2 expression. YAP, the Hippo pathway effector, is a Shh target in CGNPs and regulates IGF2 expression, and interestingly we observed that YAP is also an upstream regulator of YB-1 in Shh-induced CGNPs. Taken together, the existence of YAP/YB-1/IGF2 axis in Shh-induced CGNPs demonstrates the unique mechanism of YB-1 regulation.

Shh-signaling in CGNPs is a highly regulated process wherein proliferative signals are activated during early phase of growth and deactivated when no longer necessary; this strong regulation ensures cell homeostasis. In MBCs this regulation is compromised and leads to aberrant activation of the Shh-pathway. We observed that YB-1 is over expressed in the medulloblastomas from SmoA1 mice when compared to normal adjacent cerebellar tissue and it interacts with IGF2 promoter P3 as well. The role of this overexpression of YB-1 in medulloblastoma cell proliferation was then analysed by knockdown experimentation. As observed in case of Shh-induced CGNPs, when YB-1 expression was knocked down in SmoA1 medulloblastoma cells, there was a strong decrease in levels of proliferation markers CycD2 and PCNA, for both tumor-derived cell culture and tumor-derived organotypic slice cultures. Thus, the role of YB-1 in controlling cell proliferation is conserved both in developmental neurobiology and medulloblastoma etiology.

Our results indicate that YB-1 is required for proliferation in CGNPs and MBCs. We also observe that YB-1 is induced by Shh in CGNPs and that YAP is required for this process, suggesting the regulatory loop shown in Figure 7. Here, Shh up-regulates YAP, which is required through yet-to-be-determined mechanisms for YB-1 up-regulation. YB-1 in turn drives IGF2 expression, which results in activation of IRS1, which we have previously shown interacts with and stabilizes YAP (10). The activity of this regulatory loop, in addition to Shh-mediated N-myc and Gli induction driving their downstream gene expression programs, is an output resulting in sustained, rapid proliferation during cerebellar

development and in medulloblastoma cells. Activation of the IGF pathway is found in medulloblastomas (68) and IGF2 in particular is required for SHH-mediated medulloblastoma formation (69) *in vivo* and medulloblastoma cell proliferation *in vitro* (33). IGF1 and IGF2 activate the IGF receptor. One way through which IGF-mediated phosphoinositide-3 kinase (PI-3K) signaling cooperates with SHH signaling is by inhibiting GSK3β (14, 70), which blocks cell cycle progression in CGNPs by phosphorylating N-myc and targeting it to the proteasome for degradation.

When we searched for the expression pattern of *YBX1* (gene encoding YB-1) in human medulloblastoma genomic database, we found that *YBX1* was overexpressed in human medulloblastomas, across all subclasses. These results suggest pleiotropic roles for YB1 in the different medulloblastoma subclasses, which bear unique gene expression signatures, chromosomal aberrations, histological traits, and prognoses. However, YAP is most highly expressed in the Wnt and SHH subclasses, which IGF2 is most highly expressed in the SHH subclass, suggesting that the YAP-YB1-IGF2 relationship is unique to SHH medulloblastomas, while YB1 likely plays roles in different pathways in the other subgroups. However, due to the difference in signaling mechanisms regulating each of these subclasses and varieties we believe that the upstream regulation of YB-1 and the regulatory role of YB-1 itself in MB may be different in each subclass. Ascertaining the role of YB-1 in the other subgroups will be a fascinating area of future study, entailing the use of additional mouse models and human patient-derived xenografts that are beyond the scope of the current study.

Importantly, the regulatory loop we have described (Figure 7) contains many potential nodes for therapeutic targeting, including but not limited to Shh, IGF2, Akt, mTOR, and cdk inhibitors already in existence, and proposes YB-1 is a novel target (71) for medulloblastoma drug development. Implementation of such drug-mediated approaches to treatment have the potential to improve survival of patients as well as vastly improve quality of life for survivors, as their use may ameliorate the need for high dose radiation and chemotherapy which leave the young patients with a high risk of devastating, life-long side effects. Future studies to determine the mechanisms through which YAP regulates YB-1, identify additional pathways impacting on YB-1 expression and activity, as well as characterize functions of YB-1 beyond its transcriptional regulatory roles in cerebellar development and medulloblastoma will further expand the repertoire of approaches through which this potent network can be targeted in tumor treatment, as well as increase our understanding of the complex process of cerebellar progenitor expansion and development.

Materials and Methods

Animal Studies

Harvest of neural precursors from neonatal mice and preparation of cerebella and tumor tissue from wild-type and mutant mice for cell culture or histological analysis were carried out in compliance with the Emory University Institutional Animal Care and Use Committee guidelines. NeuroD2-SmoA1 mice were provided by Jim Olson (Fred Hutchinson Cancer Research Center). YAP-*lox*P mice were a gift from Jeff Wrana (Canada). The tumor bearing SmoA1 mice used in this study were females within an age range of 4–6 months. The wild-

type neonatal mice were not discriminated on the basis of sex to derive neural precursors and cerebellar tissue slices.

Culture of CGNPs and medulloblastoma cells

CGNP cultures were generated as described previously (Kenney and Rowitch 2000). Cells were plated on poly-DL-ornithine (Sigma, St Louis, MO, USA) precoated plates or precoated glass coverslips. Where indicated, Shh was used at a concentration of 3 μg/mL. Cyclopamine (R&D Systems, Minneapolis, MN, USA) was used at 1 μg/mL. Medulloblastoma cells (MBC) were harvested from SmoA1 mouse medulloblastomas. Briefly, tumors were disassociated and cells were incubated in Trypsin/EDTA solution for 30 minutes, then passed through a cell strainer. Cells were subsequently separated on a density step gradient of 35% and 65% Percoll solution (Sigma, St Louis, MO, USA). Purified MBCs were enriched by pre-plating on uncoated tissue culture dishes to remove adherent fibroblasts and glial cells. Non-adherent cells were plated on tissue culture dishes pre-coated with poly D-lysine (Sigma, St Louis, MO, USA) and Matrigel (BD Biosciences, San Jose, CA), infected with adenoviruses/lentiviruses 4 hours later, and cultured for 72 more hours before collection for further analysis. Mouse medulloblastoma derived PZp53Med cell line (38) was used in the ChIP experiments (below) and the cells were mycoplasma free

shRNA lentiviruses

Mission shRNA lentiviral particles (Sigma, St Louis, MO, USA) targeting YB-1 (TRCN0000077208, TRCN0000077209, TRCN0000077210, TRCN0000077211, TRCN0000222733) were purchased commercially. MISSION TRC2 pLKO.5-puro Non-Mammalian shRNA was used as a control. The efficiency of knockdown for each lentiviral plasmid was determined by adding same titre of lentiviral particles targeting YB-1 to CGNP cultures and comparing the levels of YB-1 protein with non-target shRNA (ScrShRNA) transduced CGNPs using western blotting. The batch with strongest knockdown of YB-1 (TRCN0000222733) was selected for remainder of the knockdown experiments. CGNPs were plated in medium with serum for 3 hours and then exposed to the viruses with serum-free medium +/− Shh for 24 hours. Fresh serum-free medium +/− Shh was replenished every 24 hours for the next 72 hours.

Adenovirus infection

For infection, a replication incompetent adenovirus (VectorBioLabs PA, USA, Catalog #ADV-276442/Cat# 1700,) expressing YB-1/Cre and GFP on separate promoters was used; control was GFP-only adenovirus (VectorBioLabs, Cat#1060).

Organotypic cerebellar and SmoA1 tumor slice cultures

P5 cerebella were sectioned sagittally and SmoA1 tumors were sectioned horizontally into 300-μm-thick slices with a vibratome (Lancer Vibratome Series 1000). Electroporation was performed on slices with lentiviral plasmids encoding GFP, ScrShRNA or YB-1ShRNA (Sigma Mission shRNA) using ECM 830 Square Wave Electroporation System (BTX Harvard Apparatus) with 2.5 μg of plasmid per slice. The electroporation for every slice was

done with 5 pulses of 5 ms (interval of 995 ms) at 25V. The electroporation was repeated once more with the field reversed. The slices (300 μm) were placed on trans-well inserts (1μm pore size; Falcon, Tewksbury MA, USA) precoated with poly-d-lysine and laminin and kept for 4 hours in Dulbecco's modified Eagle's medium-F-12 (DMEM/F12) (Gibco, Life Technologies, Grand Island, NY, USA) supplemented with 25 mM KCl, N2 supplement (Gibco, Life Technologies, Grand Island, NY, USA), antibiotic and 10% fetal calf serum (Sigma). After 4 hours the medium was changed to DMEM/F12/N2/KCl minus serum, with or without Shh, as indicated. The slices were cultured for 3 days, fixed in 4% paraformaldehyde on the 4th day, and immunostained with antibodies against Ki67 (Vector Biolabs, Philadelphia, PA, USA). For each experiment, three slices from three independent cerebella/tumor were analyzed by confocal microscopy (Olympus FV1000). For imaging and analysis, cerebellar boundaries were defined using DAPI staining, which allows delineation of EGL, ML, and IGL in cerebellar slices / tumor regions vs normal adjacent tissues in SmoA1-medulloblastoma slices.

Pull-down assay to identify proteins interacting with IGF2 promoters

The assay was carried out in three stages. The first stage involved preparation of lysates enriched in the nuclear fraction from tissues/cell cultures. The cells/tissues were washed with ice-cold PBS and resuspended in buffer A (20 mM Tris pH 8; 1.5 mM $MgCl_2$; 10 mM KCl, 1 mM DTT, 0.1 mM PMSF) 5 times the packed cell volume (pcv). The cells were then centrifuged at 1850g for 5 min at 4°C and re-suspended in buffer A. The cells were then lysed by 15–20 strokes in a Dounce homogenizer at 4°C. The homogenate was centrifuged at 11000g for 15 min at 4°C. The resulting nuclear pellet was re-suspended in a volume equal to half packed nuclear volume (pnv) of low salt buffer B (20 mM Tris-HCl pH 7.9 at 4°C; 25% glycerol, 1.5 mM $MgCl_2$; 0.02 M KCl; 0.2 M EDTA, 1 mM DTT, 0.1 mM PMSF) and vortexed gently. The resulting suspension was mixed ith half pnv of high salt buffer C (20 mM Tris-HCl pH 7.9 at 4°C; 25% glycerol, 1.5 mM $MgCl_2$; 1.2 M KCl; 0.2 M EDTA, 1 mM DTT, 0.1 mM PMSF) so that the final concentration of KCl is 300mM. After 2–5 strokes of further homogenization, the nuclei were extracted for 30 min with gentle mixing at 4°C. The nuclear extract was obtained as a supernatant after centrifugation at 25000g for 30 min at 4°C and stored at −20°C until the last stage of the assay. In the second stage, Igf2 promoter regions corresponding to P1 and P3 were PCR amplified from mouse genomic DNA using biotinylated primers (Supplementary Table S1) from Integrated DNA Technologies (Coralville, IA, USA). The 100bp amplicons from P1 and P3 (1 μg DNA) were immobilized on 50 μl of Dynabeads M270-streptavidin beads (Life technologies), pre-washed in buffer D (20 mM Tris-HCl pH 7.5; 1 mM EDTA; 2 M NaCl), in the same buffer D for 30 min at room temperature. The excess of buffer D was removed from the M270 beads bound to biotinylated-DNA by magnetic separation. The nuclear extract, from the first stage, was diluted to a final concentration of 0.1 M KCl and added to the M270-beads for 2 h at 4°C with gentle mixing. The unbound fraction was subsequently removed by magnetic separation and the beads were washed twice with buffer B. The promoter-bound proteins were extracted by treating the beads with high salt buffer C for 30 min at 4°C and eluting them using a magnet. The extracted samples were then subjected to either mass spectrometry or western blotting to identify proteins bound to the IGF2 promoters.

Mass spectrometry

Samples were submitted to trypsin (Promega, Madison, WI, USA) digest in 50 mM ammonium bicarbonate for 15 hrs at 37°C. Samples were dried by SpeedVac and resuspended in Buffer A (95% water, 5% acetonitrile and 0.1% formic acid) and injected for LC-MS/MS analysis on a LTQ-XL linear ion trap mass spectrometer (Thermo Fisher). Mascot (Matrix Science) version 2.3.02 was used to search against the Mouse RefV64cRapRev database. Prohits software was used to create comparative tables.

RNA extraction and RT PCR

Total RNA from CGNPs, was extracted and purified using the TRIzol reagent (Invitrogen, Life Technologies, Grand Island, NY, USA) according to manufacturer's instructions. cDNA was prepared from 1 μg of total RNA by using High-Capacity cDNA Reverse Transcription Kit (Applied Biosystems, Life Technologies, Grand Island, NY, USA) as per the maufacturer's instructions. Quantitative PCR was performed using Sso Advanced Universal SYBR green Supermix (BioRad, Hercules, CA, USA). RNA expression data were acquired using C1000 Touch Thermal Cycler and CFX96 Real-Time PCR Detection System. The data was analyzed for average results and standard errors are presented. Primers for Gli1 (Unique Assay ID: qMmuCID0026119), NMyc (Unique Assay ID: qMmuCID0009689), Bcl6 (Unique Assay ID: qMmuCID0005293), Mtss1 (Unique Assay ID: qMmuCID0012018) and GusB (Unique Assay ID: qMmuCID0046361) were purchased from BioRad. Primer sequences used for Igf2 were as follows: Igf2P3F 5′TCCTCCTCCTTCCTAGCCCCAGCG3′, Igf2P3R 5′CAGCAATGCAGCACAGAGGCGAAGCC3′.

Protein preparation and immunoblotting

Adherent and floating cells were collected, washed once with PBS, then resuspended in lysis buffer and processed as previously described (41). For each sample 30 μg were separated on 8% or 10% or 12% SDS-polyacrylamide gels and then transferred to activated PVDF membranes (Millipore). Western blotting was carried out according to standard protocols. Primary antibodies included YB-1 (Cat# 4202S), Cleaved Caspase-3 (Cat# 9664S) (Cell Signaling, Danvers, MA, USA), cyclin D2 (Cat# sc593), RAN (Cat# sc-1156) (Santa Cruz Biotechnology, Dallas, TX, USA), or β-tubulin (Cat# T4026) (Sigma, St Louis, MO, USA). Horseradish-peroxidase conjugated secondary antibodies were anti-mouse (Cat# 715-035-150, Jackson Immuno Research, West Grove, PA, USA) or anti-rabbit (Cat# 31460) Pierce, Life Technologies, Grand Island, NY, USA). Blots were developed using Amersham ECL kits. Chemiluminescence was detected by exposing membranes to GE-Amersham film for various intervals to obtain a non-saturated image.

Immunofluorescence

Paraffin-embedded sections were first de-waxed and rehydrated prior to antigen retrieval. CGNPs were grown on poly-DL-ornithine-coated glass coverslips as described previously (10). The cells were fixed with 4% paraformaldehyde for 20 min. Sections and cells were analyzed by immunofluorescence according to standard methods. Antibodies used for immunofluorescence were YB-1 (Cell Signaling Cat# 4202S/Santa Cruz Biotechnology

Cat# sc-4358), or PCNA (Calbiochem, Temecula, CA, USA; Cat# NA03), or Ki67 (Vector Labs, Burlingame, CA, USA; Cat#VP-K451), GFP (Abcam, Cambridge, MA; Cat#ab290), mouse and rabbit IgG (Life technologies; Cat# A11032, A11034, A11012, A11017).

Image capturing

Staining of cultured primary cells and tissue sections was visualized with a Leica DM2500 microscope and images were taken using Leica LFA software. For quantification, TIFF images of four random fields were taken for each experimental group using the 20× objective, and average pixel intensities were measured using ImageJ software. Confocal Images were acquired using an Olympus FV1000 laser confocal microscope and captured by Olympus Fluoview Software (Integrated Cellular Imaging Core, Emory University).

Chromatin immunoprecipitation assay

YB-1-binding sites found in 5 kb upstream of Igf2 gene were considered. ChIP was carried out with the ChIP assay kit (Millipore) according to the manufacturer's instructions. Chromatin was isolated from Pzp53 medulloblastoma cells (72) and precipitated with YB-1 antibody (73) (Abcam; Cat# ab76149), control Histone 3 antibody (Abcam; Cat# ab1791), and IgG isotype control (Upstate Biotechnologies-EMD Millipore; Cat# 12-370). Primer sequences used for quantitative PCR measurement of immunoprecipitated promotor fragments were as follows: Binding site 1 (BS1) forward, 5′-AACCCAACAGCAACAACAAA-3′; BS1 reverse, 5′-GCGACTCCATAAATGGGAAA-3′; BS2 forward, 5′-TGTTAGCCTTGGGTCACAAA-3′; BS2 reverse, 5′-TCCTTCAGGGCCAGTCTCTA-3′; BS3 forward, 5′-ACCTCCAGCATTGCTCAACT-3′; BS3 reverse, 5′-GGGGAAAGAGCATAGCAGAA-3′; No BS forward, 5′-AAACCTGCATAGACGCCTTC-3′; No BS reverse, 5′-CGAATGACACCACGCTTTTA-3′. No Binding site primers were selected 10 kb upstream of Igf2 gene, in a region that does not contain YB-1-binding sites. The remaining steps of the procedure was adopted from Fernandez etl al, 2009 (10).

Human tumor collection and imaging analysis

Gene expression analysis in previously published datasets was carried out using the R2 software (Academic Medical Center, Amsterdam, Netherlands) available at http://r2.amc.nl. Subgroup-specific expression analysis was performed in the Boston gene expression profiling dataset (2). Using the R2 software and the megasampler function (http://r2.amc.nl), we compared *YBX1* mRNA expression patterns in various gene expression profiling studies including tumor (n=1032; deposited in http://r2.amc.nl) and normal samples (n=225). The 62 medulloblastomas in the Kool et al. (74) were separated by subgroup affiliation. Expression differences were assessed using ANOVA and posthoc comparisons where appropriate. SNP6 arrays were processed, normalized, and analyzed as previously described (39, 75). Subgroup affiliation and copy number state were derived from previously published data (39, 75). The minimally overlapping region involving YBX1 was visualized in the Integrative Genomics Viewer (IGV; version 2.3). Paraffin-embedded tissue sections from a Shh-subgroup (as determined by desmoplastic histology which is unique to the Shh subgroup) medulloblastoma patient sample were obtained from Matthew Schniederjan (Children's Healthcare of Atlanta). The sections were dewaxed and rehydrated. Antigen

retrieval was performed by heating slides in sodium citrate for 20_min. After blocking endogenous peroxidases, slides were incubated with primary YB-1 antibody (Novus Biological, Littleton, CO, USA; Cat# NBP1-89945). Secondary antibodies were applied according to the manufacturer (Vector Laboratories). Slides were mounted using VectaMount permanent mounting media (Vector Laboratories). For Peptide competition assay, primary antibody for YB-1 (Novus Biologicals, NBP1-89945) dilution was prepared at usual concentration of 0. 5 ng/μL and YBX1-blocking peptide (Abcam, ab175051) was added at a concentration of 5ng/μL. Antibody/peptide dilution was incubated at one hour at room temperature before being used in lieu of primary antibody for immunostaining.

Sample Size and quantitation

The sample size was chosen based on our previous report (44). All experiments for CGNP proliferation assessment were repeated using pups from five separate litters. Each litter comprised of an average of 12 mice. Immunochemistry experiments were performed with five coverslips per treatment/infection, for each litter. Five randomly selected fields of 100 cells per coverslip were analyzed by an unbiased observer, using DAPI staining to select homogeneously distributed cell fields. Thus, statistical depiction of data are representative of a total n=20, 100-cell fields. Data are shown as percentage change from Shh-treated GFP-infected cultures. GFP infected cultures did not differ from uninfected Shh-treated cultures in levels of proliferation (not shown). For cerebellar slice cultures, experiments were performed using pups from three separate litters. With each separate litter, three slices were used for each electroporation. Data represented in graphs are from n=9 experiments. For primary cell cultures derived from SmoA1 medulloblastoma tissue, the proliferation evaluation was repeated on 6 mice with tumors per condition. The imaging based quantification was same as in case of CGNPs (mentioned previously) with n=20, 100-cell fields. The SmoA1 tumor slice culture experiments were derived from three different mice bearing tumors. The mice bearing tumors were selected based on symptoms described by Jim Olson and colleagues (15). With each separate mouse, three slices were used for each electroporation. Data represented in graphs are from n=9 experiments. Error bars represent standard deviation of the mean. Significance (P>0.01 in comparison with Shh-treated uninfected/GFP-infected CGNPs) was determined using the two-tailed t-test (Excel software). For RT-PCR and immunoblot analysis, two wells per treatment were pooled to maximize recovery of RNA and protein. Experiments for those analyses were repeated with three separate litters. Simple randomization was employed in all experiments where randomization is based on a single sequence of random assignments (control versus treated) (76).

Supplementary Material

Refer to Web version on PubMed Central for supplementary material.

Acknowledgments

We are grateful for the resources available from the Winship Cancer Institute (WCI)-Pathology Core Lab for paraffin embedding of tissues. We acknowledge the assistance provided by Neil Anthony (Integrated Imaging Core, Emory University) during image acquisition and analysis. We thank Tobey Macdonald, Matthew Schniederjan and Megan Hamling from Children's Healthcare of Atlanta (CHOA) for providing human medulloblastoma tissue

sections. We also thank Daniel Brat and Carol Tucker-Burden for assistance in slice culture experiments. We greatly appreciated suggestions and feedback from Nada Jabado, Dan Brat, Sandra Dunn, Tracy Ann-Read, Renee Read, and Tamara Caspary.

Funding

This work has been supported by grants to AMK from the NIH (NINDS R01 NS061070), CURE Childhood Cancer Foundation, and Winship Cancer Institute (P30 center grant-CA138292). AD acknowledges Alex Lemonade Stand Foundation and Northwestern Mutual Foundation for Young Investigator Award and Imaging studies were supported by a pilot grant to AD from the Integrated Cellular Imaging (ICI) core at Emory University.

References

1. Packer RJ, Cogen P, Vezina G, Rorke LB. Medulloblastoma: clinical and biologic aspects. Neuro-oncology. 1999; 1(3):232–50. [PubMed: 11550316]
2. Cho YJ, Tsherniak A, Tamayo P, Santagata S, Ligon A, Greulich H, et al. Integrative genomic analysis of medulloblastoma identifies a molecular subgroup that drives poor clinical outcome. Journal of clinical oncology : official journal of the American Society of Clinical Oncology. 2011; 29(11):1424–30. [PubMed: 21098324]
3. Northcott PA, Korshunov A, Witt H, Hielscher T, Eberhart CG, Mack S, et al. Medulloblastoma comprises four distinct molecular variants. Journal of clinical oncology : official journal of the American Society of Clinical Oncology. 2011; 29(11):1408–14. [PubMed: 20823417]
4. Pomeroy SL, Cho YJ. Molecular fingerprints of medulloblastoma and their application to clinical practice. Future Oncol. 2011; 7(3):327–9. [PubMed: 21417897]
5. Eberhart CG. Even cancers want commitment: lineage identity and medulloblastoma formation. Cancer Cell. 2008; 14(2):105–7. [PubMed: 18691544]
6. Dahmane N, Ruiz i Altaba A. Sonic hedgehog regulates the growth and patterning of the cerebellum. Development. 1999; 126(14):3089–100. [PubMed: 10375501]
7. Wallace VA. Purkinje-cell-derived Sonic hedgehog regulates granule neuron precursor cell proliferation in the developing mouse cerebellum. Curr Biol. 1999; 9(8):445–8. [PubMed: 10226030]
8. Wechsler-Reya RJ, Scott MP. Control of neuronal precursor proliferation in the cerebellum by Sonic Hedgehog. Neuron. 1999; 22(1):103–14. [PubMed: 10027293]
9. Bhatia B, Northcott PA, Hambardzumyan D, Govindarajan B, Brat DJ, Arbiser JL, et al. Tuberous sclerosis complex suppression in cerebellar development and medulloblastoma: separate regulation of mammalian target of rapamycin activity and p27 Kip1 localization. Cancer research. 2009; 69(18):7224–34. [PubMed: 19738049]
10. Fernandez LA, Northcott PA, Dalton J, Fraga C, Ellison D, Angers S, et al. YAP1 is amplified and up-regulated in hedgehog-associated medulloblastomas and mediates Sonic hedgehog-driven neural precursor proliferation. Genes Dev. 2009; 23(23):2729–41. [PubMed: 19952108]
11. Parathath SR, Mainwaring LA, Fernandez LA, Campbell DO, Kenney AM. Insulin receptor substrate 1 is an effector of sonic hedgehog mitogenic signaling in cerebellar neural precursors. Development. 2008; 135(19):3291–300. [PubMed: 18755774]
12. Fernandez LA, Squatrito M, Northcott P, Awan A, Holland EC, Taylor MD, et al. Oncogenic YAP promotes radioresistance and genomic instability in medulloblastoma through IGF2-mediated Akt activation. Oncogene. 2012; 31(15):1923–37. [PubMed: 21874045]
13. Mainwaring LA, Kenney AM. Divergent functions for eIF4E and S6 kinase by sonic hedgehog mitogenic signaling in the developing cerebellum. Oncogene. 2011; 30(15):1784–97. [PubMed: 21339731]
14. Kenney AM, Widlund HR, Rowitch DH. Hedgehog and PI-3 kinase signaling converge on Nmyc1 to promote cell cycle progression in cerebellar neuronal precursors. Development. 2004; 131(1): 217–28. [PubMed: 14660435]
15. Hatton BA, Villavicencio EH, Tsuchiya KD, Pritchard JI, Ditzler S, Pullar B, et al. The Smo/Smo model: hedgehog-induced medulloblastoma with 90% incidence and leptomeningeal spread. Cancer research. 2008; 68(6):1768–76. [PubMed: 18339857]

16. Hu JF, Vu TH, Hoffman AR. Differential biallelic activation of three insulin-like growth factor II promoters in the mouse central nervous system. Mol Endocrinol. 1995; 9(5):628–36. [PubMed: 7565809]

17. Lasham A, Print CG, Woolley AG, Dunn SE, Braithwaite AW. YB-1: oncoprotein, prognostic marker and therapeutic target? The Biochemical journal. 2013; 449(1):11–23. [PubMed: 23216250]

18. Shibao K, Takano H, Nakayama Y, Okazaki K, Nagata N, Izumi H, et al. Enhanced coexpression of YB-1 and DNA topoisomerase II alpha genes in human colorectal carcinomas. International journal of cancer Journal international du cancer. 1999; 83(6):732–7. [PubMed: 10597187]

19. Gimenez-Bonafe P, Fedoruk MN, Whitmore TG, Akbari M, Ralph JL, Ettinger S, et al. YB-1 is upregulated during prostate cancer tumor progression and increases P-glycoprotein activity. The Prostate. 2004; 59(3):337–49. [PubMed: 15042610]

20. Oda Y, Sakamoto A, Shinohara N, Ohga T, Uchiumi T, Kohno K, et al. Nuclear expression of YB-1 protein correlates with P-glycoprotein expression in human osteosarcoma. Clinical cancer research : an official journal of the American Association for Cancer Research. 1998; 4(9):2273–7. [PubMed: 9748149]

21. Kamura T, Yahata H, Amada S, Ogawa S, Sonoda T, Kobayashi H, et al. Is nuclear expression of Y box-binding protein-1 a new prognostic factor in ovarian serous adenocarcinoma? Cancer. 1999; 85(11):2450–4. [PubMed: 10357417]

22. Yahata H, Kobayashi H, Kamura T, Amada S, Hirakawa T, Kohno K, et al. Increased nuclear localization of transcription factor YB-1 in acquired cisplatin-resistant ovarian cancer. Journal of cancer research and clinical oncology. 2002; 128(11):621–6. [PubMed: 12458343]

23. Gu C, Oyama T, Osaki T, Kohno K, Yasumoto K. Expression of Y box-binding protein-1 correlates with DNA topoisomerase IIalpha and proliferating cell nuclear antigen expression in lung cancer. Anticancer research. 2001; 21(4A):2357–62. [PubMed: 11724293]

24. Shibahara K, Sugio K, Osaki T, Uchiumi T, Maehara Y, Kohno K, et al. Nuclear expression of the Y-box binding protein, YB-1, as a novel marker of disease progression in non-small cell lung cancer. Clinical cancer research : an official journal of the American Association for Cancer Research. 2001; 7(10):3151–5. [PubMed: 11595709]

25. Oda Y, Ohishi Y, Saito T, Hinoshita E, Uchiumi T, Kinukawa N, et al. Nuclear expression of Y-box-binding protein-1 correlates with P-glycoprotein and topoisomerase II alpha expression, and with poor prognosis in synovial sarcoma. The Journal of pathology. 2003; 199(2):251–8. [PubMed: 12533839]

26. Bargou RC, Jurchott K, Wagener C, Bergmann S, Metzner S, Bommert K, et al. Nuclear localization and increased levels of transcription factor YB-1 in primary human breast cancers are associated with intrinsic MDR1 gene expression. Nature medicine. 1997; 3(4):447–50.

27. Janz M, Harbeck N, Dettmar P, Berger U, Schmidt A, Jurchott K, et al. Y-box factor YB-1 predicts drug resistance and patient outcome in breast cancer independent of clinically relevant tumor biologic factors HER2, uPA and PAI-1. International journal of cancer Journal international du cancer. 2002; 97(3):278–82. [PubMed: 11774277]

28. Rubinstein DB, Stortchevoi A, Boosalis M, Ashfaq R, Guillaume T. Overexpression of DNA-binding protein B gene product in breast cancer as detected by in vitro-generated combinatorial human immunoglobulin libraries. Cancer research. 2002; 62(17):4985–91. [PubMed: 12208750]

29. Huang J, Tan PH, Li KB, Matsumoto K, Tsujimoto M, Bay BH. Y-box binding protein, YB-1, as a marker of tumor aggressiveness and response to adjuvant chemotherapy in breast cancer. International journal of oncology. 2005; 26(3):607–13. [PubMed: 15703814]

30. Wu J, Lee C, Yokom D, Jiang H, Cheang MC, Yorida E, et al. Disruption of the Y-box binding protein-1 results in suppression of the epidermal growth factor receptor and HER-2. Cancer research. 2006; 66(9):4872–9. [PubMed: 16651443]

31. Faury D, Nantel A, Dunn SE, Guiot MC, Haque T, Hauser P, et al. Molecular profiling identifies prognostic subgroups of pediatric glioblastoma and shows increased YB-1 expression in tumors. Journal of clinical oncology : official journal of the American Society of Clinical Oncology. 2007; 25(10):1196–208. [PubMed: 17401009]

32. Pham NV, Nguyen MT, Hu JF, Vu TH, Hoffman AR. Dissociation of IGF2 and H19 imprinting in human brain. Brain research. 1998; 810(1–2):1–8. [PubMed: 9813220]
33. Hartmann W, Koch A, Brune H, Waha A, Schuller U, Dani I, et al. Insulin-like growth factor II is involved in the proliferation control of medulloblastoma and its cerebellar precursor cells. Am J Pathol. 2005; 166(4):1153–62. [PubMed: 15793295]
34. Chowdhury RP, Gupta S, Chatterji D. Identification and characterization of the dps promoter of Mycobacterium smegmatis: promoter recognition by stress-specific extracytoplasmic function sigma factors sigmaH and sigmaF. J Bacteriol. 2007; 189(24):8973–81. [PubMed: 17921287]
35. Zhang C, Basta T, Jensen ED, Klymkowsky MW. The beta-catenin/VegT-regulated early zygotic gene Xnr5 is a direct target of SOX3 regulation. Development. 2003; 130(23):5609–24. [PubMed: 14522872]
36. Gall JG, Bellini M, Wu Z, Murphy C. Assembly of the nuclear transcription and processing machinery: Cajal bodies (coiled bodies) and transcriptosomes. Molecular biology of the cell. 1999; 10(12):4385–402. [PubMed: 10588665]
37. Rotwein P, Hall LJ. Evolution of insulin-like growth factor II: characterization of the mouse IGF-II gene and identification of two pseudo-exons. DNA Cell Biol. 1990; 9(10):725–35. [PubMed: 1702294]
38. Berman DM, Karhadkar SS, Hallahan AR, Pritchard JI, Eberhart CG, Watkins DN, et al. Medulloblastoma growth inhibition by hedgehog pathway blockade. Science. 2002; 297(5586): 1559–61. [PubMed: 12202832]
39. Northcott PA, Shih DJ, Peacock J, Garzia L, Morrissy AS, Zichner T, et al. Subgroup-specific structural variation across 1,000 medulloblastoma genomes. Nature. 2012; 488(7409):49–56. [PubMed: 22832581]
40. Brunet A, Datta SR, Greenberg ME. Transcription-dependent and -independent control of neuronal survival by the PI3K-Akt signaling pathway. Curr Opin Neurobiol. 2001; 11(3):297–305. [PubMed: 11399427]
41. Kenney AM, Rowitch DH. Sonic hedgehog promotes G(1) cyclin expression and sustained cell cycle progression in mammalian neuronal precursors. Molecular and cellular biology. 2000; 20(23):9055–67. [PubMed: 11074003]
42. Corrales JD, Rocco GL, Blaess S, Guo Q, Joyner AL. Spatial pattern of sonic hedgehog signaling through Gli genes during cerebellum development. Development. 2004; 131(22):5581–90. [PubMed: 15496441]
43. Bai CB, Auerbach W, Lee JS, Stephen D, Joyner AL. Gli2, but not Gli1, is required for initial Shh signaling and ectopic activation of the Shh pathway. Development. 2002; 129(20):4753–61. [PubMed: 12361967]
44. Kenney AM, Cole MD, Rowitch DH. Nmyc upregulation by sonic hedgehog signaling promotes proliferation in developing cerebellar granule neuron precursors. Development. 2003; 130(1):15–28. [PubMed: 12441288]
45. En-Nia A, Yilmaz E, Klinge U, Lovett DH, Stefanidis I, Mertens PR. Transcription factor YB-1 mediates DNA polymerase alpha gene expression. The Journal of biological chemistry. 2005; 280(9):7702–11. [PubMed: 15615704]
46. Uchiumi T, Fotovati A, Sasaguri T, Shibahara K, Shimada T, Fukuda T, et al. YB-1 is important for an early stage embryonic development: neural tube formation and cell proliferation. The Journal of biological chemistry. 2006; 281(52):40440–9. [PubMed: 17082189]
47. Miwa A, Higuchi T, Kobayashi S. Expression and polysome association of YB-1 in various tissues at different stages in the lifespan of mice. Biochimica et biophysica acta. 2006; 1760(11):1675–81. [PubMed: 17045744]
48. Eliseeva IA, Kim ER, Guryanov SG, Ovchinnikov LP, Lyabin DN. Y-box-binding protein 1 (YB-1) and its functions. Biochemistry Biokhimiia. 2011; 76(13):1402–33. [PubMed: 22339596]
49. Finkbeiner MR, Astanehe A, To K, Fotovati A, Davies AH, Zhao Y, et al. Profiling YB-1 target genes uncovers a new mechanism for MET receptor regulation in normal and malignant human mammary cells. Oncogene. 2009; 28(11):1421–31. [PubMed: 19151767]

50. Tiberi L, Bonnefont J, van den Ameele J, Le Bon SD, Herpoel A, Bilheu A, et al. A BCL6/BCOR/SIRT1 complex triggers neurogenesis and suppresses medulloblastoma by repressing Sonic Hedgehog signaling. Cancer Cell. 2014; 26(6):797–812. [PubMed: 25490446]
51. Callahan CA, Ofstad T, Horng L, Wang JK, Zhen HH, Coulombe PA, et al. MIM/BEG4, a Sonic hedgehog-responsive gene that potentiates Gli-dependent transcription. Genes & development. 2004; 18(22):2724–9. [PubMed: 15545630]
52. Lee J, Platt KA, Censullo P, Ruiz i Altaba A. Gli1 is a target of Sonic hedgehog that induces ventral neural tube development. Development. 1997; 124(13):2537–52. [PubMed: 9216996]
53. Fernandez LA, Squatrito M, Northcott P, Awan A, Holland EC, Taylor MD, et al. Oncogenic YAP promotes radioresistance and genomic instability in medulloblastoma through IGF2-mediated Akt activation. Oncogene. 2011
54. Reginensi A, Scott RP, Gregorieff A, Bagherie-Lachidan M, Chung C, Lim DS, et al. Yap- and Cdc42-dependent nephrogenesis and morphogenesis during mouse kidney development. PLoS genetics. 2013; 9(3):e1003380. [PubMed: 23555292]
55. Wu J, Stratford AL, Astanehe A, Dunn SE. YB-1 is a Transcription/Translation Factor that Orchestrates the Oncogenome by Hardwiring Signal Transduction to Gene Expression. Transl Oncogenomics. 2007; 2:49–65. [PubMed: 23641145]
56. Grant CE, Deeley RG. Cloning and characterization of chicken YB-1: regulation of expression in the liver. Molecular and cellular biology. 1993; 13(7):4186–96. [PubMed: 8321222]
57. Sabath DE, Podolin PL, Comber PG, Prystowsky MB. cDNA cloning and characterization of interleukin 2-induced genes in a cloned T helper lymphocyte. The Journal of biological chemistry. 1990; 265(21):12671–8. [PubMed: 2142689]
58. Ito K, Tsutsumi K, Kuzumaki T, Gomez PF, Otsu K, Ishikawa K. A novel growth-inducible gene that encodes a protein with a conserved cold-shock domain. Nucleic acids research. 1994; 22(11):2036–41. [PubMed: 8029009]
59. Stenina OI, Poptic EJ, DiCorleto PE. Thrombin activates a Y box-binding protein (DNA-binding protein B) in endothelial cells. The Journal of clinical investigation. 2000; 106(4):579–87. [PubMed: 10953033]
60. Lossi L, Alasia S, Salio C, Merighi A. Cell death and proliferation in acute slices and organotypic cultures of mammalian CNS. Progress in neurobiology. 2009; 88(4):221–45. [PubMed: 19552996]
61. Lee JE, Pintar J, Efstratiadis A. Pattern of the insulin-like growth factor II gene expression during early mouse embryogenesis. Development. 1990; 110(1):151–9. [PubMed: 1964408]
62. Jurchott K, Bergmann S, Stein U, Walther W, Janz M, Manni I, et al. YB-1 as a cell cycle-regulated transcription factor facilitating cyclin A and cyclin B1 gene expression. The Journal of biological chemistry. 2003; 278(30):27988–96. [PubMed: 12695516]
63. Mertens PR, Harendza S, Pollock AS, Lovett DH. Glomerular mesangial cell-specific transactivation of matrix metalloproteinase 2 transcription is mediated by YB-1. The Journal of biological chemistry. 1997; 272(36):22905–12. [PubMed: 9278454]
64. Uchiumi T, Kohno K, Tanimura H, Matsuo K, Sato S, Uchida Y, et al. Enhanced expression of the human multidrug resistance 1 gene in response to UV light irradiation. Cell growth & differentiation : the molecular biology journal of the American Association for Cancer Research. 1993; 4(3):147–57. [PubMed: 8466853]
65. Lasham A, Lindridge E, Rudert F, Onrust R, Watson J. Regulation of the human fas promoter by YB-1, Puralpha and AP-1 transcription factors. Gene. 2000; 252(1–2):1–13. [PubMed: 10903433]
66. Lasham A, Moloney S, Hale T, Homer C, Zhang YF, Murison JG, et al. The Y-box-binding protein, YB1, is a potential negative regulator of the p53 tumor suppressor. The Journal of biological chemistry. 2003; 278(37):35516–23. [PubMed: 12835324]
67. Homer C, Knight DA, Hananeia L, Sheard P, Risk J, Lasham A, et al. Y-box factor YB1 controls p53 apoptotic function. Oncogene. 2005; 24(56):8314–25. [PubMed: 16158057]
68. Reiss K. Insulin-like growth factor-I receptor - a potential therapeutic target in medulloblastomas. Expert Opin Ther Targets. 2002; 6(5):539–44. [PubMed: 12387677]
69. Hahn H, Wojnowski L, Specht K, Kappler R, Calzada-Wack J, Potter D, et al. Patched target Igf2 is indispensable for the formation of medulloblastoma and rhabdomyosarcoma. The Journal of biological chemistry. 2000; 275(37):28341–4. [PubMed: 10884376]

70. Mill P, Mo R, Hu MC, Dagnino L, Rosenblum ND, Hui CC. Shh controls epithelial proliferation via independent pathways that converge on N-Myc. Dev Cell. 2005; 9(2):293–303. [PubMed: 16054035]

71. Dolfini D, Mantovani R. Targeting the Y/CCAAT box in cancer: YB-1 (YBX1) or NF-Y? Cell Death Differ. 2013; 20(5):676–85. [PubMed: 23449390]

72. Corcoran RB, Bachar Raveh T, Barakat MT, Lee EY, Scott MP. Insulin-like growth factor 2 is required for progression to advanced medulloblastoma in patched1 heterozygous mice. Cancer research. 2008; 68(21):8788–95. [PubMed: 18974121]

73. Jung K, Wu F, Wang P, Ye X, Abdulkarim BS, Lai R. YB-1 regulates Sox2 to coordinately sustain stemness and tumorigenic properties in a phenotypically distinct subset of breast cancer cells. BMC Cancer. 2014; 14:328. [PubMed: 24885403]

74. Kool M, Koster J, Bunt J, Hasselt NE, Lakeman A, van Sluis P, et al. Integrated genomics identifies five medulloblastoma subtypes with distinct genetic profiles, pathway signatures and clinicopathological features. PLoS ONE. 2008; 3(8):e3088. [PubMed: 18769486]

75. Shih DJ, Northcott PA, Remke M, Korshunov A, Ramaswamy V, Kool M, et al. Cytogenetic prognostication within medulloblastoma subgroups. Journal of clinical oncology : official journal of the American Society of Clinical Oncology. 2014; 32(9):886–96. [PubMed: 24493713]

76. Suresh K. An overview of randomization techniques: An unbiased assessment of outcome in clinical research. J Hum Reprod Sci. 2011; 4(1):8–11. [PubMed: 21772732]

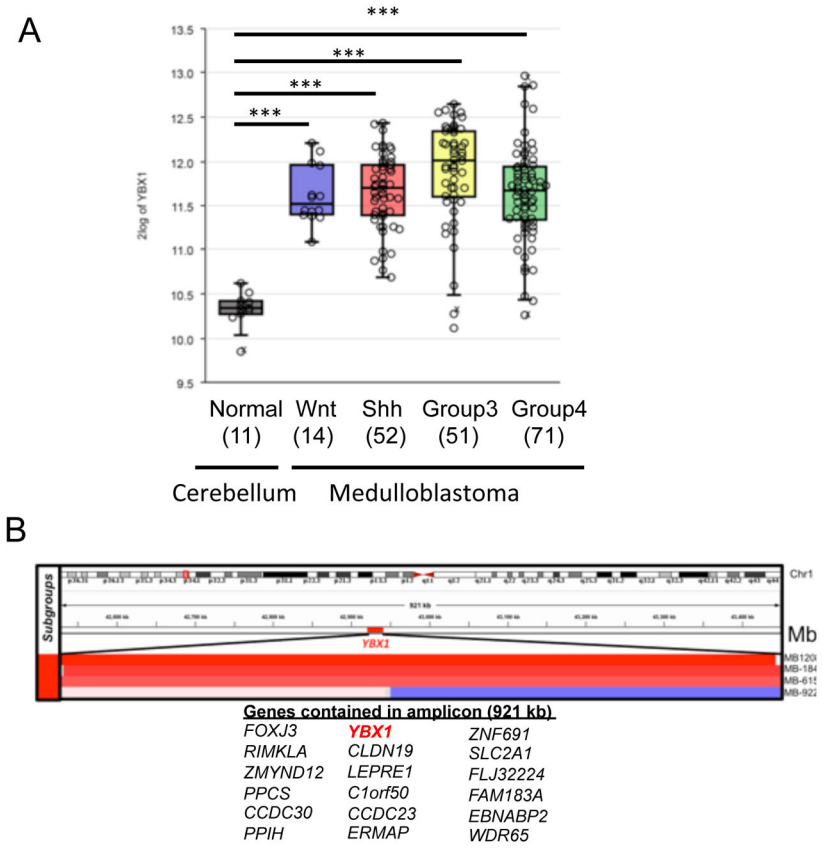

Figure 1.

YB-1 is highly overexpressed in all sub-groups of human medulloblastomas YB-1 is amplified in all subsets of human medulloblastomas. (*a*) Box plot showing *YBX1* mRNA expression from an exon array profiling of 188 human medulloblastomas and 11 cerebella. *YBX1* is highly expressed in Wnt-, Shh-, Group 3 and Group 4 medulloblastomas. These plots are a useful means of presenting differences between populations (i.e. medulloblastoma subgroups) as they display groups of numerical data (in this case, signal intensity/expression level of *YBX1* gene in adult cerebellum and medulloblastoma subgroups) through their five number summaries: the smallest observation (sample minimum= lower line), lower quartile (Q1 = bottom of box), median (Q2= line in box), upper quartile (Q3= top of the box), and largest observation (sample maximum= upper line). These plots can also identify any observations that may represent outliers (circles outside the boxes). YB-1 is amplified in all subclasses of human medulloblastomas (Normal cerebellum Vs Wnt $p=4.9 \times 10^{-11}$; Normal cerebellum Vs Shh $p=1.9 \times 10^{-14}$; Normal cerebellum Vs Group 3 $p=1.3 \times 10^{-12}$; Normal cerebellum Vs Group 4 $p=4.9 \times 10^{-11}$; Normal cerebellum Vs Wnt $p=1.1 \times 10^{-11}$); (*b*) Focal amplification and copy number gains harbouring *YBX1* were observed in 4/1088 medulloblastomas, all of which belonged to the SHH subgroup (SHH-MB affiliation is depicted by red blocks next to the copy number heatmap; all genes encompassed in the minimally overlapping region enlisted in the lower panel). The minimally overlapping region involving *YBX1* was visualized in the Integrative Genomics Viewer (IGV; version 2.3)

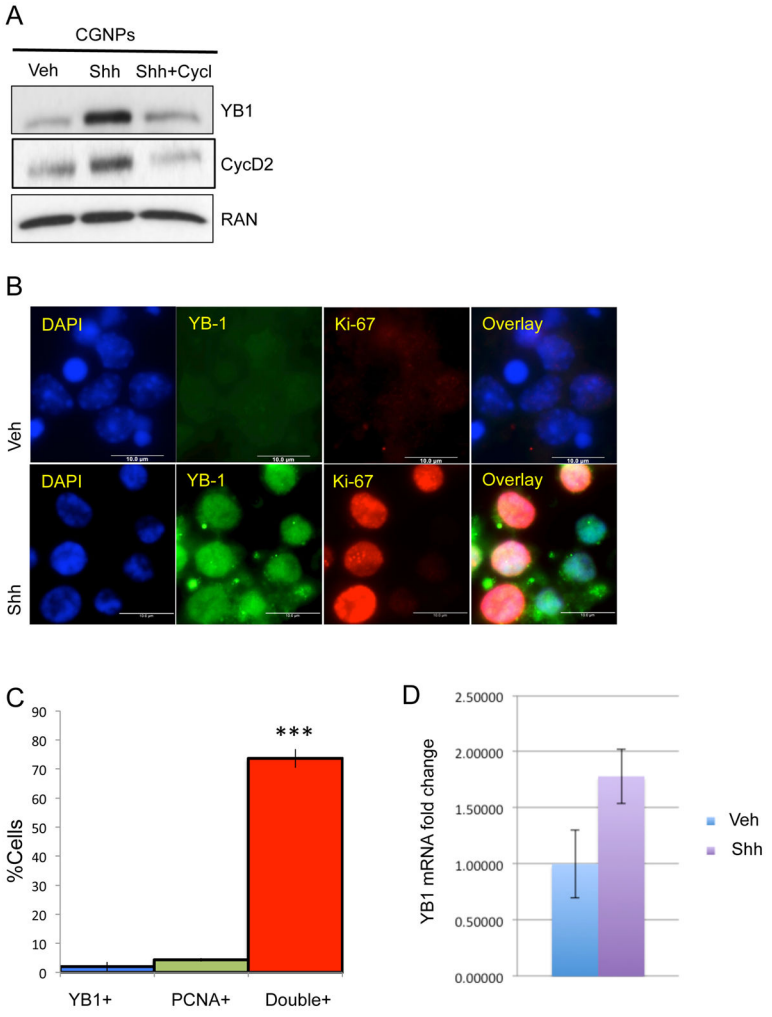

Figure 2.

YB-1 protein expression is up-regulated by Shh. (*a*) CGNPs were cultured in vitro for 48 h in the presence or absence of Shh, then treated with cyclopamine for 12 h when indicated. (*b*) CGNPs cultured in the absence or presence of Shh were fixed and immunostained for YB-1 and Ki67 (Scale bar = 50 μm). (*c*) Percentage of cells expressing Ki67, YB-1, or both ($p<0.001$). (*D*) YB-1 mRNA level change in the presence of Shh is insignificant in CGNPs.

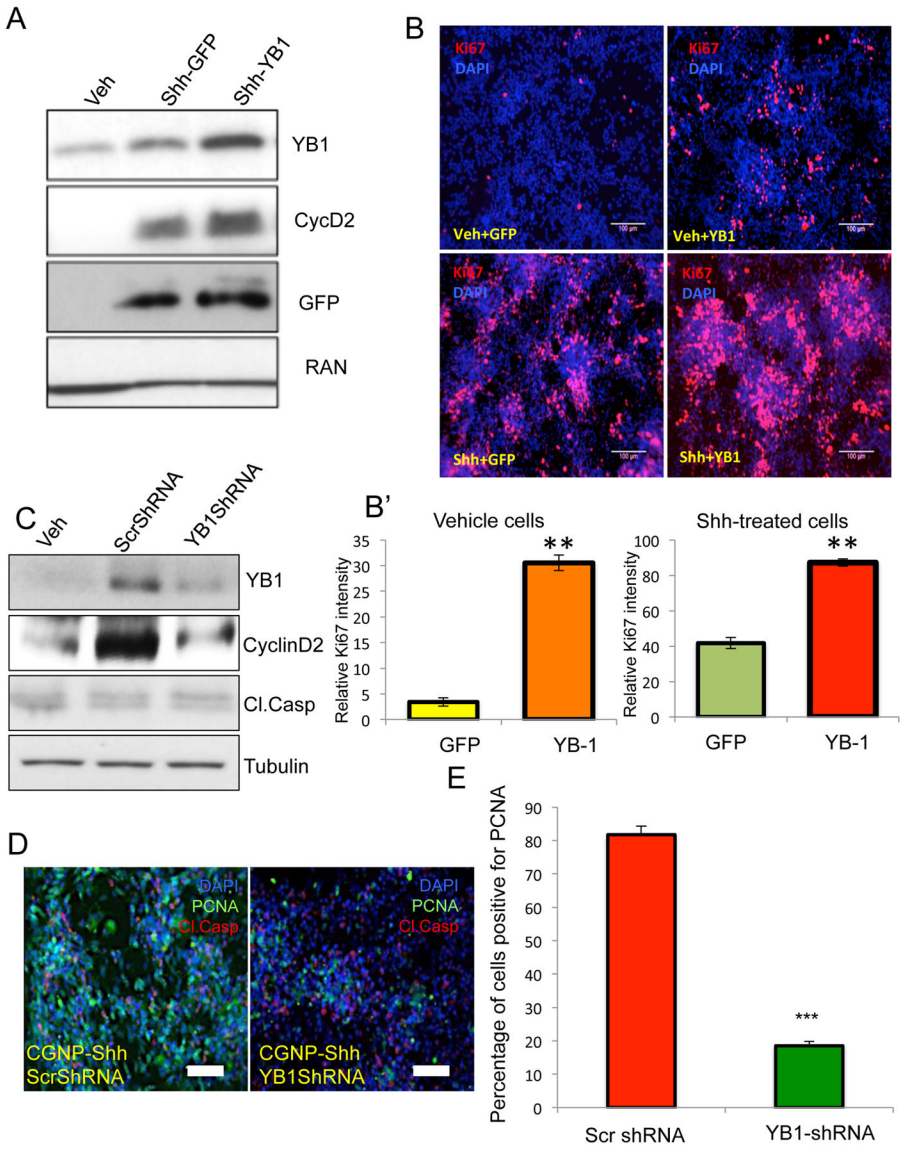

Figure 3.

YB-1 regulates proliferation in CGNPs. (*a*) Western blot showing increase in YB-1 protein levels when CGNPs were infected with adenoviruses expressing YB-1. CyclinD2 levels increased as result of YB-1 overexpression. *(b)* CGNPs were transduced with YB-1 expressing adenoviruses. Cells were immunostained for Ki67. (Top; Left) In the absence of Shh and presence of GFP-expressing adenovirus few cells proliferate. When YB-1 is overexpressed in absence of Shh, proliferation increases (Top; Right), although not to the same extent as in the presence of Shh and GFP-expressing adenovirus (Bottom; Left). Overexpression of YB-1 in the presence of Shh leads to increased proliferation of CGNPs. *(b′)* Quantification of Ki67 staining in Figure 3b using Image J shows significant ($p<0.01$) difference in Ki67 positive cells when over-expressing YB-1, both in presence and absence of Shh, compared to control (GFP); *(c)* Western blot showing a strong reduction in YB-1 protein levels when CGNPs were infected with YB-1 shRNA lentiviruses. CyclinD2 levels

were dramatically decreased with no observable change in cleaved caspase3. *(d)* PCNA immunostaining in CGNPs infected with YB-1 shRNAs shows a decrease in proliferation compared with control shRNA-infected cells (Scale bar = 50 μm); (*e*) Automated quantification of PCNA staining in CGNPs transduced with ScrShRNA or YB-1 ShRNA lentiviruses. F different fields were considered in each case. Statistically significant differences are indicated as (**) $p < 0.01$; (***) $p < 0.001$.

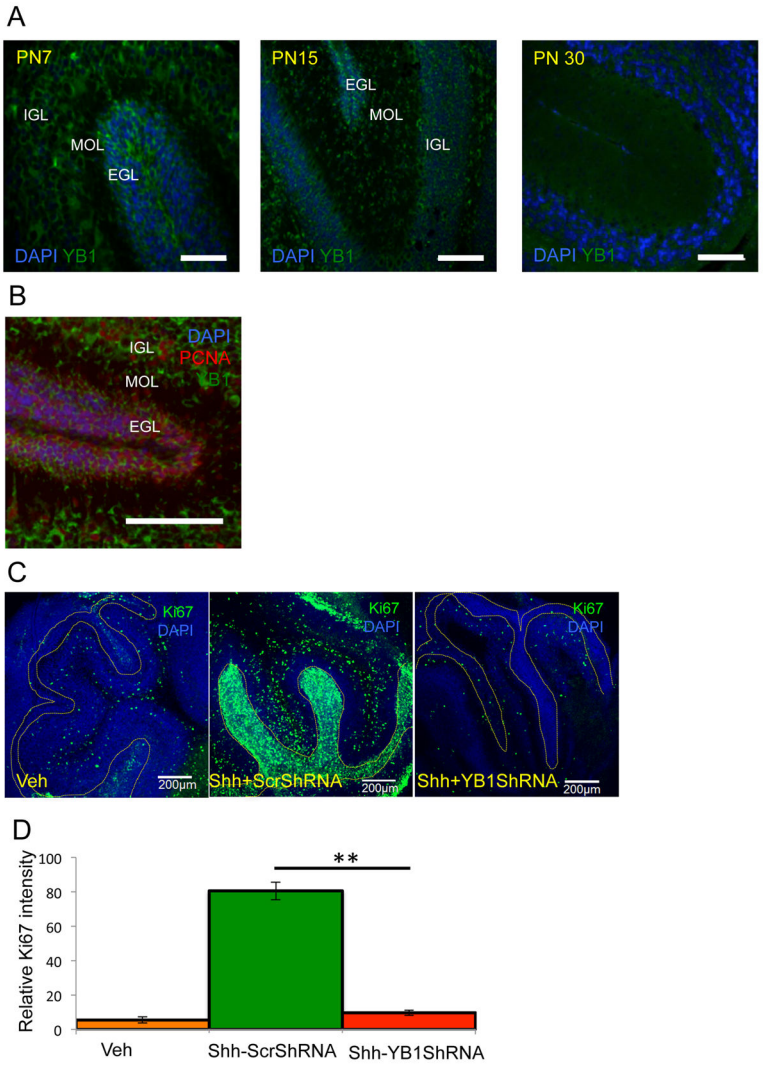

Figure 4.

Downregulation of YB-1 leads to reduced proliferation from EGL *ex vivo. (a)* Cerebella of SW129 mice were immunostained for YB-1 at three developmental stages. At PN7, YB-1 is expressed mainly in the EGL. (*Middle*) At PN15, YB-1 is present in granule cells in the IGL, and in their processes in the molecular layer. In adult cerebella, we could not detect YB-1 protein (Scale bar = 50 μm). (*b*) Immunostaining of wild type PN7 sagittal cerebellar sections. YB-1 (green) is elevated in the EGL and co-expresses with the proliferation marker PCNA (red) (Scale bar = 50 μm). (*c*) Electroporation of cerebellar slices with lentiviral plasmids targeting YB-1 causes reduced thickness of the EGL (yellow dotted lines) and reduced Ki67 staining (green) in the EGL. In the representative images, Blue represents DAPI counterstaining. (Scale bar = 100 μm). (*d*) Automated quantification of Ki67 staining in postnatal day 7 cerebellar slice cultures electroporated with ScrShRNA or YB-1 ShRNA plasmids. Three different fields were considered in each image within the EGL (dotted lines). The analysis was repeated for three cerebellar samples from three different wild-type Crl-CD1(ICR) mice. Statistically significant differences are indicated as (**) $p < 0.01$; (***) $p < 0.001$.

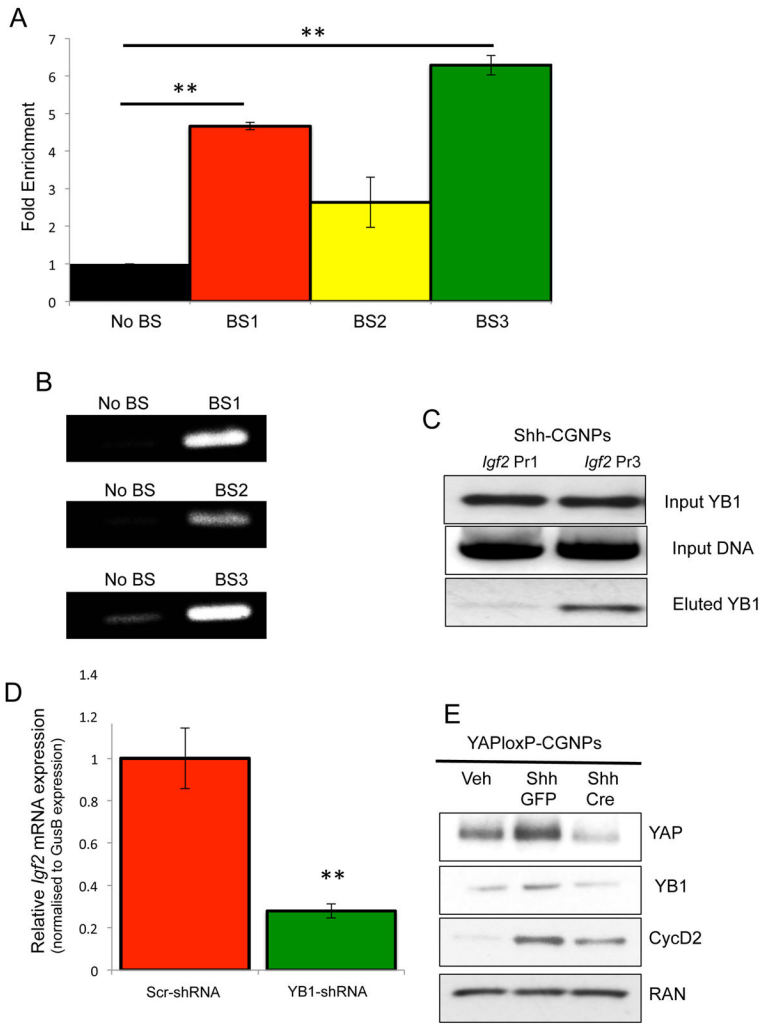

Figure 5.

YB-1 regulates IGF2 transcription in CGNPs (*a*) To test the presence of YB-1 on IGF2 promoter ChIP assay was carried out. Three regions containing YB-1 binding sites were tested. Fold enrichments normalized to the level observed at the control region are shown. Statistically significant differences are shown as (*) $p < 0.05$; (**) $p < 0.01$; (***) $p < 0.001$ *(b)* Results of PCR amplification of ChIP assay from the 3 binding site (BS) regions when compared to non-binding site (No BS) regions. *(c)* IGF2 promoter-specific pull-down analysis shows YB-1 interacting with IGF2 promoter P3 in Shh-induced CGNPs. (*d*) YB-1 knockdown in Shh-induced CGNPs significantly reduces the expression of IGF2 as measured by quantitative RT-PCR ($p < 0.01$). (*e*) Cre-mediated ablation of YAP in CGNPs derived from cerebella of P5 YAP-*loxP* mice showed reduced YB-1 and CycD2 protein levels as determined by western blot.

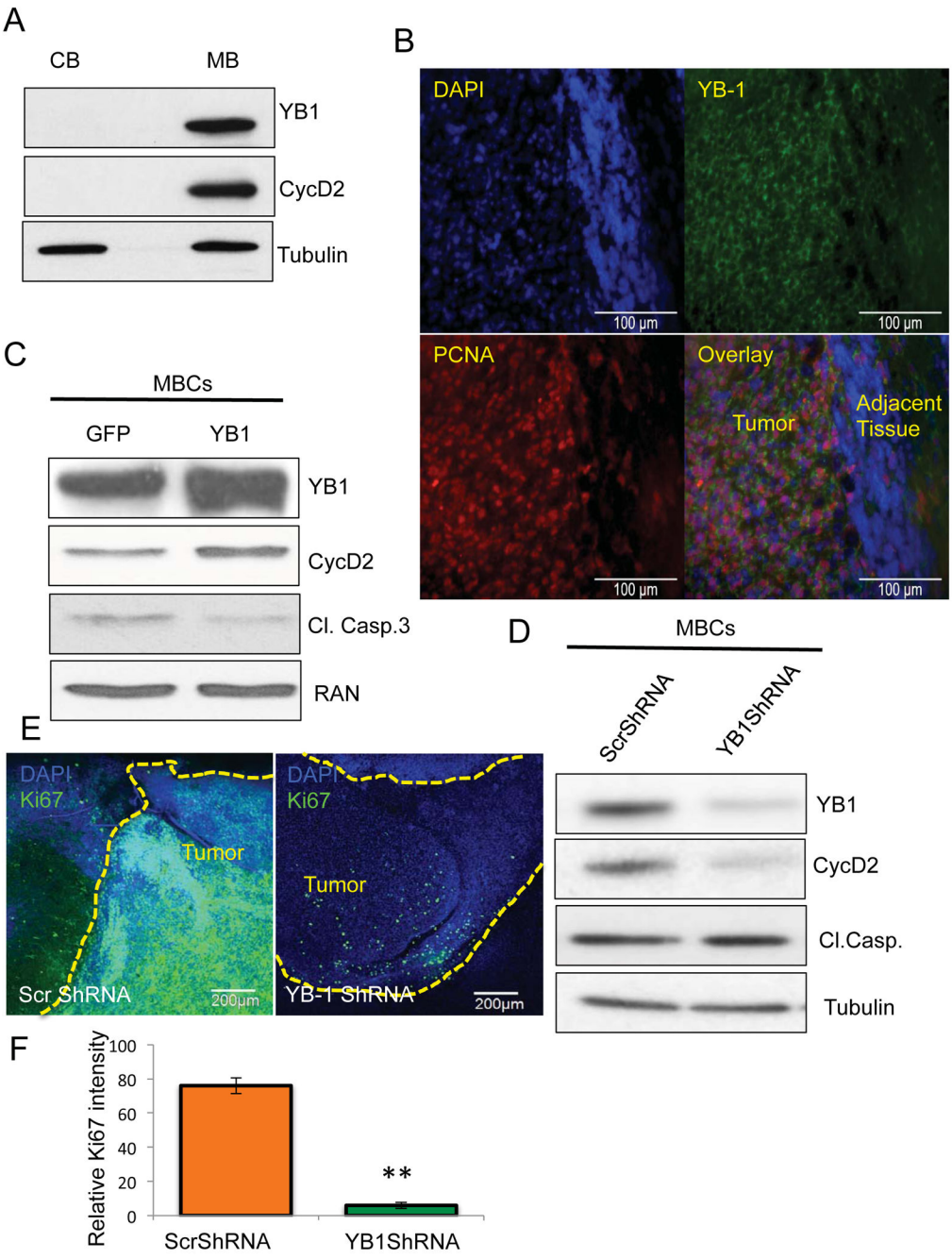

Figure 6.

YB-1 is highly expressed in mouse medulloblastomas and its manipulation controls proliferation. *a*) Western blot showing high levels of YB-1 in medulloblastomas from *NeuroD2-SmoA1* transgenic animals. The comparison of Shh-induced CGNPs vs SmoA1 tumor tissues are shown in Supplementary figure 8C. (*b*) Immunostaining for YB-1 and PCNA in tumor sections from *NeuroD2-SmoA1* transgenic animals shows high levels of YB-1 in tumor regions as compared to adjacent tissue. (*c*) Western blot showing the over-expression of YB-1 in MBCs increases proliferation (CycD2 levels). (*d*) Western blot

showing a strong reduction in YB-1 protein levels when MBCs were infected with YB-1 shRNA lentiviruses. CyclinD2 levels were dramatically decreased with no observable change in cleaved caspase 3. Quantitative estimation of YB-1 knockdown in MBCs is shown in supplementary figure S8B. (*e*) Electroporation of SmoA1 tumor with lentiviral plasmids targeting YB-1 causes reduced Ki67 staining (green) in the tumor region (yellow dotted lines). Blue represents DAPI counterstaining (Scale bar = 200 μm). *(f)* Automated quantification of Ki67 staining in SmoA1 tumor slice cultures electroporated with ScrShRNA or YB-1 ShRNA plasmids. Three different fields were considered in each image within the tumor region (yellow dotted lines). The analysis was repeated for three different tumor samples from three different SmoA1 mice per condition (Scr- Vs YB-1 shRNA). Statistically significant differences are indicated as (**) $p < 0.01$; (***) $p < 0.001$.

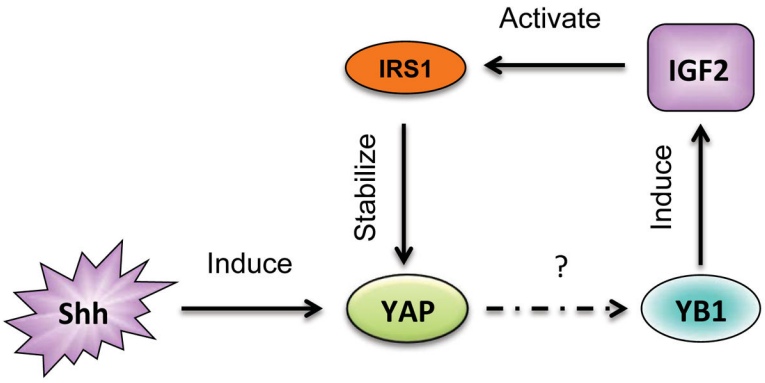

Figure 7.

Model of regulatory loop between Shh, IRS1, YAP, and YB1. Shh pathway leads to YB-1 upregulation. YB-1 controls IGF2 expression. IGF2 activates IRS1, which is stabilized by Shh, and in turn stabilizes YAP (10, 11). YAP regulates IGF2 expression downstream of Shh and could be an upstream regulator of YB-1.